Asian Journal of Chemistry; Vol. 24, No. 10 (2012), 4633-4637

ASIAN JOURNAL OF CHEMISTRY

www.asianjournalofchemistry.co.in

Chlorine Adsorption Characteristics of NaX, NaY and Mordenite Zeolites

JIAN-WEI XUE, HUI-LING ZHAO, HUI WANG, FU-XIANG LI and ZHI-PING LV*

Research Institute of Special Chemicals, Taiyuan University of Technology, Taiyuan 030024, Shanxi Province, P.R. China

*Corresponding author: Fax: +86 351 6111178; Tel: +86 351 6010550-3; E-mail: zhipinglv@yeah.net

(*Received*: 17 August 2011; *Accepted*: 9 May 2012) AJC-11454

This paper examines the potential of zeolites as ideal chlorine adsorption materials. The NaX, NaY and mordenite zeolites, a large class of highly crystalline aluminosilicate materials that encompass well-defined channels and cavities, were investigated and compared according to their chlorine adsorption properties. The chlorine adsorption capacities were measured by a pressure-composition-temperature experimental setup and the data were obtained at a temperature range of 273-323 K and pressures in the range of 0-0.35 MPa. At 273 K and 0.317 MPa, the maximum adsorption capacity was 29.02 % for the NaY zeolite, 28.96 % for the mordenite zeolite and 21.03 % for the NaX zeolite. The experimental data show that the chlorine uptakes in the zeolites are strongly dependent on temperature and pressure, as well as on the framework and aperture type.

Key Words: Chlorine, NaX, NaY, Mordenite zeolite, Adsorption.

INTRODUCTION

The characteristics of chlorine adsorption are extensively investigated because of its great importance in chemical industries. Chlorine gas is an aggressive chemical used in various industries and can be produced as part of the end product or a reactant in various processes ranging from plastics to tap-water purification[1]. The main production route for chlorine is by the electrolysis of brine in the chlor-alkali process. The chlor-alkali industry is the backbone of inorganic chemical field and considerable chlorine tail gas is produced in the process of chlorine utilization and reaction. Because of the hazard posed by this gas to human health and the environment, the improvement of processes and devices involving this gas is necessary.

This work focuses on the use of zeolites as an alternative method to adsorb chlorine gas reversibly and efficiently in an ultrahigh vacuum system. Among the best-known microporous solids, zeolites have the advantages of high stability, low cost and a variety of porous structures[2]. Zeolites have received increasing attention from the chemical and petroleum industries for use in a wide range of processes. The unique structure and chemistry of these microporous materials have led to their application in such areas as ion-exchange, drying purification, catalysis and separation by selective adsorption[3]. For example, molecular sieve was used in CO_2 removing from N_2[4]. However, despite the well-established usage of these materials for adsorption and separation, limited studies have been conducted regarding the chlorine adsorption properties of zeolites[5]. These applications have provided an early incentive for both theoretical[6] and experimental[7,8] studies on the adsorption of a range of gases (*e.g.*, Ar, Xe, Kr, N_2) on zeolite materials. Of particular interest is the variation in the size and charge of the exchangeable cations. Experimental data have shown that the most important factors for adsorption capacity, including temperature, pressure, surface area, pore volume, channel size, SiO_2/Al_2O_3 ratio, affect the chlorine absorption capability of microporous materials. In the design of an adsorption based separation process, the choice of the adsorbent is the most crucial design consideration[9-11]. Considering these parameters, many zeolites with large pore volume and suitable channel diameter have not been investigated for their adsorption properties. Here, the authors identify the characteristics of the adsorption of chlorine gas on NaX, NaY and mordenite zeolites by examining adsorption capacities.

EXPERIMENTAL

The materials used in the experiments (*i.e.*, NaX, NaY and mordenite zeolites) were of industrial grade. The potassium iodide solution of different concentrations to determine the residual chlorine content, 0.1 mol/L sodium thiosulfate solution and 10 g/L starch reagent were prepared in the authors' laboratory. The 99.9 % pure chlorine and 99.5 % pure nitrogen gases were of industrial grade. The main instruments used were vacuum pumps, intelligent temperature controller, single-punch tablet press and muffle furnace.

The crystallization framework structures and phase purity of the zeolites were measured by Rigaku D/2500 X-ray diffractometer (XRD) using copper K_α radiation, where Cu targets K_α as the X-ray source and scanning ranged from 5-45° under 40 kV voltage and 100 mA current. The surface area and pore properties of zeolites were analyzed through nitrogen physisorption at 77.4 K. The skeleton structures of the zeolites measured with the Shimadzu FT-IR-8400S infrared spectrometer were detected under the frequency 4500-350 cm^{-1}. The morphological data were acquired through scanning electron microscopy (SEM) on JSM-6360 LV manipulated at 10 kV.

Experimental setup: The pressure-composition-temperature (P-C-T) experimental setup for the adsorption process is shown in Fig. 1. Here, P_1 represents the instructions source pressure of the chlorine gas; P_2 is the precision pressure gauge for the range 0-1.6 MPa (gauge pressure); P_3 is the vacuum gauge range -0.1-0 MPa (vacuum); D represents the dry filter tube within the silica gel, anhydrous calcium chloride; F_1-F_6 are the copper valves and G is the drying device composited by silica gel and NaA zeolite.

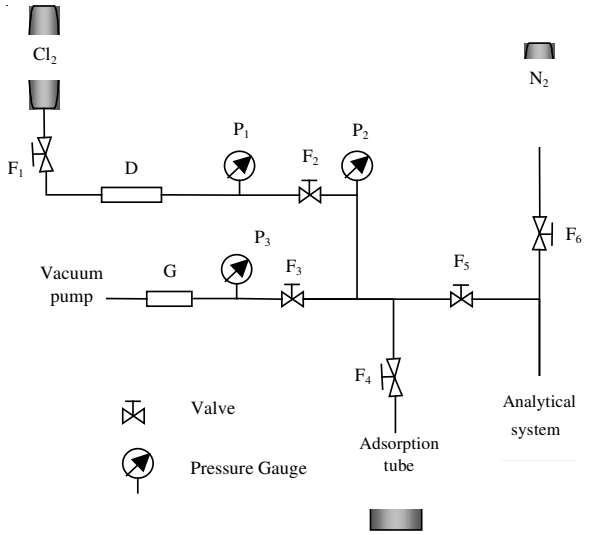

Fig. 1. P-C-T experimental setup for adsorption process study

Methods: The adsorption equilibrium data for chlorine on each material were measured by the P-C-T experimental setup mentioned as in Fig. 1. The samples were activated in the muffle furnace at 823 K for 4 h and then placed in an adsorption tube to complete the activation process at 423 K for 2 h under vacuum. The samples were allowed to cool to room temperature for the adsorption process. All the data obtained in this process were used to determine the adsorption curves for analysis and further studies.

RESULTS AND DISCUSSION

X-Ray powder diffraction analysis of zeolite samples before and after chlorine adsorption: The XRD method was employed for measuring the phase of the samples. The XRD patterns of the three zeolites before and after chlorine adsorption are shown in Fig. 2. The diffraction peaks in the patterns of the NaX zeolite shifted to a lower value after adsorption. The chlorine atoms may have been absorbed by Si-OH or

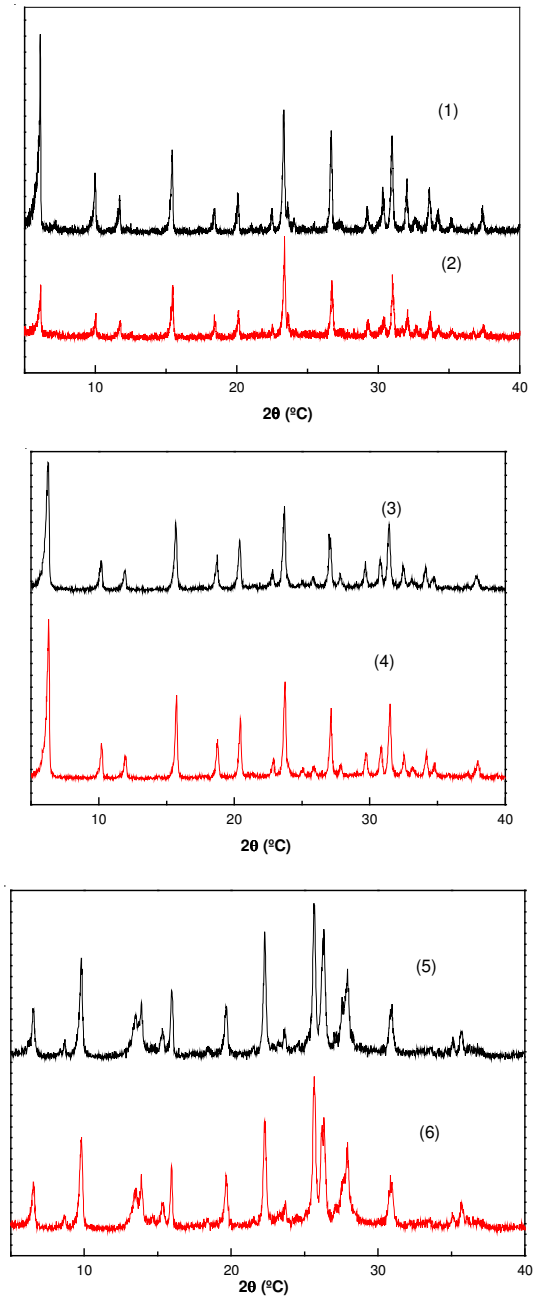

Fig. 2. XRD patterns of NaX, NaY and mordenite before and after chlorine adsorption. (1) NaX before adsorption (2) NaX after adsorption (3) NaY before adsorption (4) NaY after adsorption (5) mordenite zeolite before adsorption (6) mordenite zeolite after adsorption

Al-OH on the surface of the NaX zeolite. Meanwhile, the intensities of the main peaks decreased after adsorption, suggesting less uniform mesopores compared with those before adsorption.

Hence, based on the data included in curves (3)-(6) in Fig. 2, no NaY and mordenite structural disintegration occurred due to the chlorine adsorption. The diffraction peaks were narrow and their distribution occurred at the same angle values. The results show evidence of small changes in the structures of the NaY and mordenite zeolites before and after adsorption. Furthermore, these patterns indicate that the NaY and mordenite zeolites were more stable than the NaX zeolite. Thus, the diffraction peak positions and relative diffraction intensities of the sample are consistent with the standard data

for the three zeolites[12]. Comparing the experimental data with the standard data[12] proved that the industrial products were also eligible.

Infrared spectral analysis of zeolite samples before and after chlorine adsorption: The infrared spectra of the NaX, NaY and mordenite zeolites before and after chlorine adsorption are presented in Fig. 3. The FT-IR spectrum of the NaX zeolite is shown in Fig. 3(a). The wavenumber at 365 cm^{-1}, which is considered as a characteristic fingerprint of the twelve-member ring orifice of the fausite (FAU) structure, also revealed the high crystallinity of the NaX zeolite. The peaks found at 580-550 cm^{-1} were the characteristic adsorption bands of the double six-member ring of NaX zeolite. The absorption peak at 980 cm^{-1} was affected by the collective vibration of the Si-O-Al, representing the basic skeleton of the NaX zeolite.

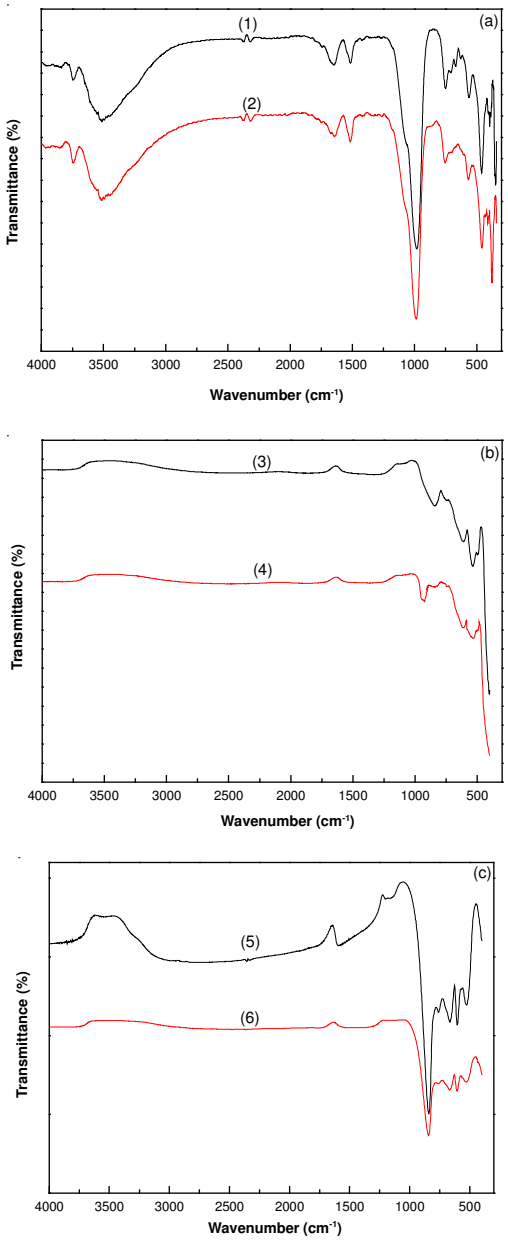

Fig. 3. Infrared spectra of NaX, NaY and mordenite zeolites before and after chlorine adsorption. (a) NaX; (b) NaY; (c) mordenite (1) NaX before adsorption (2) NaX after adsorption (3) NaY before adsorption (4) NaY after adsorption (5) mordenite zeolite before adsorption (6) mordenite zeolite after adsorption

The FT-IR spectrum of the NaY zeolite presented in Fig. 3(b) shows that the band at 450 cm^{-1} is the T-O deformation vibration of the inner tetrahedron that is insensitive to the structure. The appearance of a very weak band at 578 cm^{-1} is attributed to the double-ring external linkage peak associated with the fausite structure[13]. The bands at 720-650 cm^{-1} are the symmetrical stretching vibrations of the tetrahedral inner links and the bands at 1250-950 cm^{-1} are the asymmetrical stretching vibrations of the tetrahedral outer links. The bands of the skeleton vibration are consistent with previous literature.

The spectrum of the mordenite zeolite is illustrated in Fig. 3(c). The bands around 1226 and 1050 cm^{-1} are the T-O of the in-plane and out-of-plane asymmetrical stretching vibrations, respectively. The wavenumber around 800 cm^{-1} shows the bands of the T-O of the in-plane and out-of-plane symmetrical stretching vibrations, whereas the bands around the wavenumber at 557 and 627 cm^{-1} are either the vibrations of the five-member ring or are five-member ring related. The band at 447 cm^{-1} is the T-O deformation vibration. The band at 585 cm^{-1}, assigned to the five-member ring vibrations and which is very sensitive to structure, did not change. A reduction and/or shift of the bands at 1226 cm^{-1}, which is attributed to the asymmetrical stretching between the tetrahedral[14] and 627 and 557 cm^{-1}, which are related to the presence of the different ring types in the mordenite structures[15], are indications of loss in crystallinity[16,17], likely as a consequence of dealumination. Therefore, the FT-IR spectra corroborate the proposed hypothesis mentioned above and suggest that the loss in crystallinity was due to the partial destruction of the zeolites structure.

Scanning electron microscopy analysis: The size and morphology of the zeolite crystallites were determined by SEM. The micrographs of NaX, NaY and mordenite zeolites are presented in Fig. 4. The SEM images show that NaX and NaY zeolites have the typical fausite framework, which are found as highly porous small single crystals. The images also indicate the presence of small nearly globular particles of irregular sizes. The NaX and NaY zeolites are cubic crystals, consistent with the literature[18]. The SEM image of the mordenite zeolite, showing a tufted, amorphous and fibrous structure, is illustrated in Fig. 4(c). The different grain and pore dimensions are likely the main reasons for the heterogeneous distribution of the chlorine molecules on the mordenite surface.

Effects of temperature on chlorine adsorption of NaX, NaY and mordenite zeolites: The isotherms of the chlorine adsorption of NaX, NaY and mordenite zeolites at different temperatures are depicted in Fig. 5. The zeolites adsorption curves conform to the Langmuir's adsorption and the isotherms are considered to conform to physisorption. The adsorption capacities increased when the temperature decreased, whereas the adsorption capacities decreased. Compared with the NaX and mordenite zeolites, the chlorine adsorption capacity of NaY zeolite is the strongest and can reach 29.02 % at 273 K and 0.317 MPa. As the pressure decreased, the adsorption capacities declined substantially, likely because of the level of chlorine liquefaction under its saturated vapour pressure of 368.92 KPa at 273 K.

Chlorine adsorption capacities of NaX, NaY and mordenites at 303 K: The chlorine adsorption isotherms of the three different zeolites are displayed by Fig. 6. The

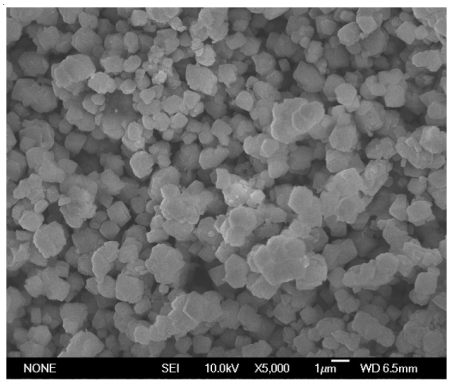

(a)

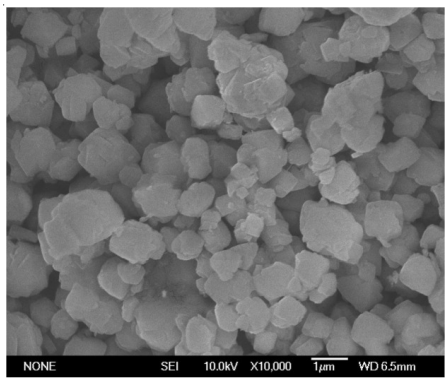

(b)

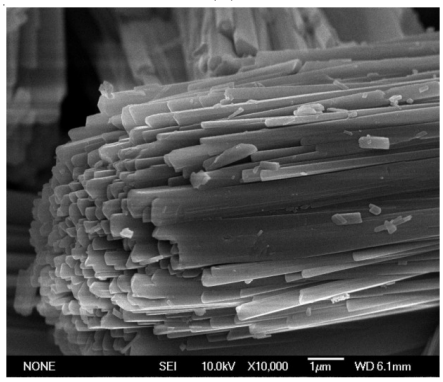

(c)

Fig. 4. SEM images of the zeolites (a) NaX; (b) NaY; (c) mordenite zeolite

isotherms show that the adsorption capacities of the zeolites increased as the pressure increased. According to the experimental data, the highest chlorine adsorption capacities for the NaX, NaY and mordenite zeolites were 17.10, 21.85 and 25.12 %, respectively, at 303 K and 0.317 MPa. These results signify that the NaY zeolite had a higher adsorption capacity than the two other zeolites.

The framework schemes of the three zeolites from the Atlas of zeolite framework types[19] are shown in Fig. 7. The NaX and NaY zeolites exhibit fausite structure, indicating that they are three-dimensional channel materials and they have twelve-ring channels and super-cages connected with the main channels. At the same time, they have the same silicon (aluminum) oxygen skeleton, while the different atomic ratio of Si:Al, which is one of the reasons caused two kinds of zeolites have different adsorption forces on chlorine. In addition, different SiO_2/Al_2O_3 ratio of zeolites will lead to different gas adsorption capacity. SiO_2/Al_2O_3 ratio of NaY zeolite is larger

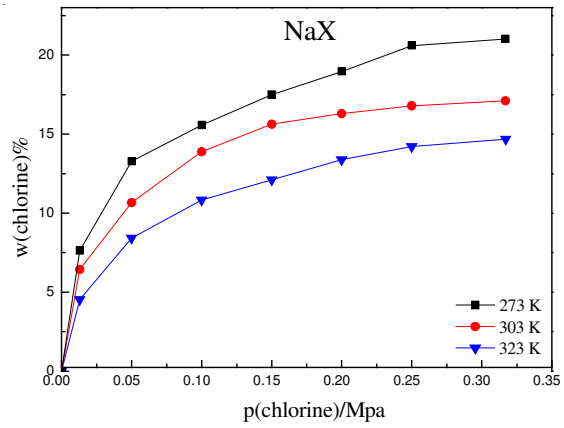

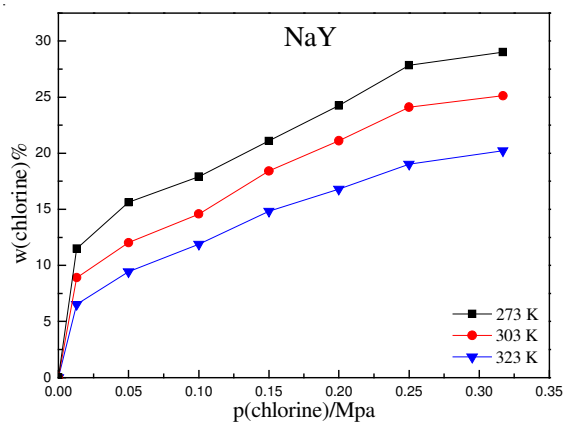

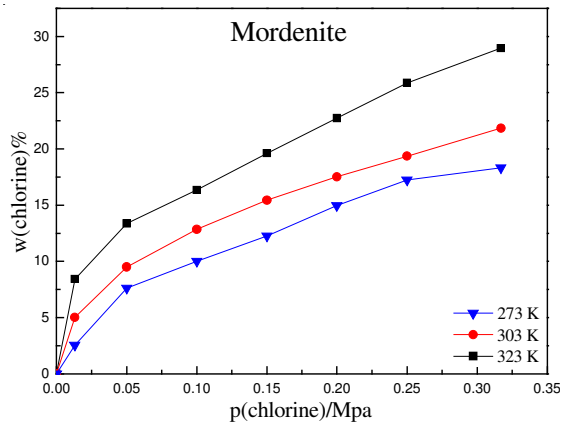

Fig. 5. Chlorine adsorption isotherms of NaX, NaY and mordenite zeolites

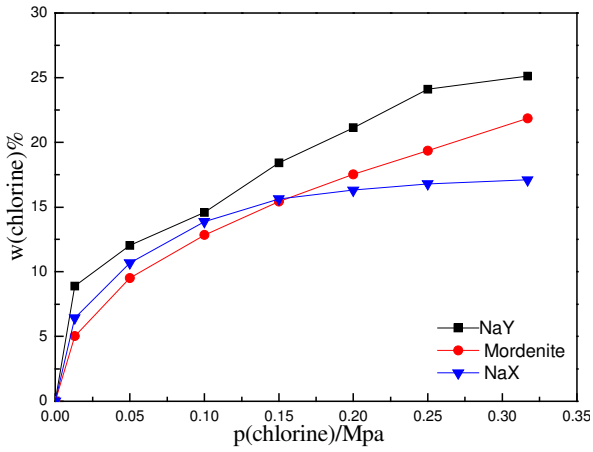

Fig. 6. Chlorine adsorption isotherms of different zeolites at 303 K

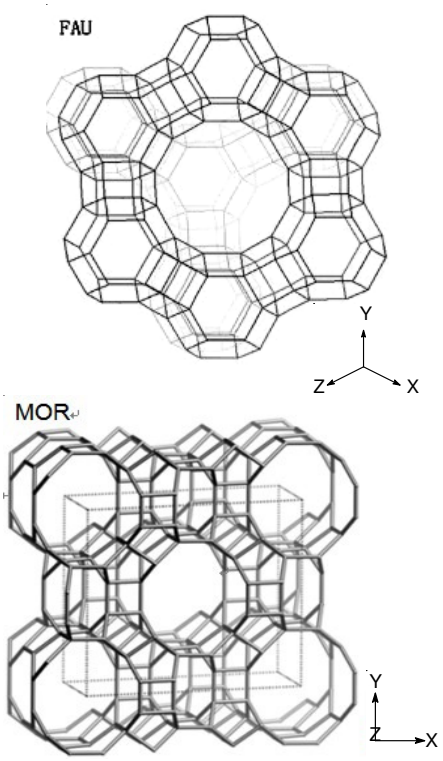

Fig. 7. Schematic representations of a super cell of the fausite (FAU) and mordenite zoelite (MOR)

than that of NaX zeolite (Table-1), the higher the SiO_2/Al_2O_3 ratio, the lower the polarity[4]. Chlorine molecules belong to the polarity molecules, so NaY zeolite with lower polarity is better than the NaX zeolite on chlorine molecules adsorption performance. In contrast, mordenite zeolite has a two-dimensional channel materials similarly, SiO_2/Al_2O_3 ratio of mordenite zeolite is 10 (Table-1), which has lower polarity and better chlorine molecules adsorption performance than that of NaX zeolite. However, the main pore size and the side pore size of mordenite zeolite are 0.65 nm × 0.70 nm and 0.26 nm × 0.51 nm[20], therefore, chlorine molecules whose kinetic diameter is 0.44 nm is difficult to access their side of the channel. Meanwhile, the molecular dynamics diameter of the best adsorption pore diameter of zeolite is 2-6 times[21,22]. NaY zeolite whose pore diameter is 0.8-0.9 consist with its best adsorption pore, therefore, although the SiO_2/Al_2O_3 ratio of mordenite zeolite is larger than that of NaY zeolite, adsorption capacity of NaY zeolite on chlorine is still greater than that of mordenite zeolite.

TABLE-1
PHYSICAL PROPERTIESOF DIFFERENT TYPES OF ADSORBENTS

Adsorbent	Pore size (nm)	Pore volume (cm^3/g)	SiO_2/Al_2O_3 ratio	Surface area (m^2/g)
NaY	0.8-0.9	0.35	4.5-5.0	900
NaX	0.9-1	0.34	2.5	950
Mordenite	0.26-0.7	0.20	10-13	400

Conclusion

The chlorine adsorption capacities of the zeolites are determined by the external (temperature and pressure) and internal (framework and aperture) factors, which have been interpreted in this work. The maximum adsorption capacity of the NaY zeolite was 29.02 % at 273 K and 0.317 MPa. The results show that a large adsorption capacity for chlorine by physisorption at a low temperature and high pressure results from the large cage in the framework, appropriate channel size and pore volume. The optimal zeolite materials have the better chlorine adsorption capacities under the suitable conditions of temperature and pressure than other adsorbents, indicating a wider range of applications. However, the stability and durability of these materials need to be improved.

ACKNOWLEDGEMENTS

The authors, Jianwei Xue and Huiling Zhao thank Shanxi Natural Science Foundation Committee for financial support. This work has been supported by Shanxi Natural Science Foundation Committee Under No. 200811025: Study for characteristics of the molecular sieve adsorption chlorine.

REFERENCES

1. A. Lindbrathen and M.B. Hagg, *Chem. Eng. Process.,* **48**, 1 (2009).
2. K.P. Prasanth, R.S. Pillai, S.A. Peter, H.C. Bajaj, R.V. Jasra, H.D. Chung, T.H. Kim and S.D. Song, *J. Alloy Compd.,* **466**, 439 (2008).
3. D.M. Razmus and C.K. Hall, *AIChE J.,* **37**, 769 (1991).
4. P.J.E. Harlick and F.H. Tezel, *Micropor. Mesopor. Mater.,* **76**, 71 (2004).
5. R.M. Barrer, Zeolites and Clay Minerals as Sorbents and Molecular Sieves, Academic Press, London (1978).
6. D. Fraenkel, *J. Chem. Soc. Faraday Trans. I*, **77**, 2041 (1981).
7. D.R. Corbin, L. Abrams, G.A. Jones, M.L. Smith, C.R. Dybowski, J.A. Hriljac and J.B. Parise, *J. Chem. Soc., Chem. Commun.,* 1027 (1993).
8. S. Bordiga, G.T. Palomino, C. Paze and A. Zecchina, *Micropor. Mesopor. Mater.,* **34**, 67 (2000).
9. R. Kumar, *Ind. Eng. Chem. Res.,* **33**, 1600 (1994).
10. R. Kumar, *Adsorption,* **1**, 203 (1995).
11. D.M. Ruthven, S. Farooq and K. Knaebel, Pressure Swing Adsorption, VCH Publishers, New York (1994).
12. M.M.J. Treacy, J.B. Higgins and B.J. Higgins, Collection of Simulated XRD Powder Patterns for Zeolites, Amsterdam, Elsevier (2001).
13. D.M. Ginter, A.T. Bell and C.J. Radke, *Zeolites,* **12**, 742 (1992).
14. G.P. Giannetto, Zeolitas: Caracteristicas, Propiedadesy Aplicaciones Industriales, Caracas: Editorial Innovacion Tecnologica (1990).
15. W. Mozgawa, *J. Mol. Struct.*, **596**, 129 (2001).
16. M. Lezcano, A. Ribotta, E. Miró, E. Lombardo, J. Petunchi, C. Moreaux and J.M. Dereppe, *J. Catal.,* **168**, 511 (1997).
17. M. Handke and W. Mozgawa, *Vib. Spectrosc.*, **5**, 75 (1993).
18. S.Y. Yang, Q.H. Li, M.J. Wang and A. Navrotsky, *Micropor. Mesopor. Mater.*, **87**, 261 (2006).
19. Ch. Baerlocher, W.M. Meier and D.H. Olson, Atlas of Zeolite Framework Types, Amsterdam: Elsevier, pp. 132-133, 190-191 (2001).
20. H.Y. Huang, J. Padin and R.T. Yang, *Ind. Eng. Chem. Res.*, **38**, 2720 (1999).
21. T. Zan and E. Gubbinsk, *J. Phys. Chem*., **94**, 6061 (1990).
22. Y. Zou, Z. Wu, S. Lu and Y. Zhu, *Chem. Eng. Oil Gas*, **26**, 15 (1997).